

$A$  along the  $x$  axis, the solid line in Fig. 7 is shown again in Fig. 8. Figure 7 was the result for 5 cm of thickness and Fig. 8 that for 2.5 cm thickness. As a result, we can say that while the advanced phase shift is independent of the length of the resonance tube along the  $y$  axis, it is affected by the thickness of the resonance tube along the  $x$  axis.

Furthermore, the phase shift advances with increasing thickness, and if we shift one of the solid lines in Fig. 8 by a factor of  $\frac{1}{2}$  or the other by a factor of 2 in the molecular concentration, then the two lines coincide. This indicates that the corresponding time constant  $T_e$  varies as  $T_e \propto (nA)^{1/2}$ , where  $n$  is molecular concentration.

Figure 9 shows the angular dependence of the phase shift for observation along directions other than the  $x$  and  $y$  axes. This result was obtained using a half-cylindrical resonance tube. A smooth transition occurred from advanced to retarded phase.

Also, we examined the dependence on carrier amplitude and frequency, on the modulation factor  $m$  in Eq. (1), on the amplitude of the modulated wave, on the effects of the weak electric and magnetic fields, and on the use of polarized light waves. These factors gave

only small or null effects on the phenomenon which causes the advanced phase shift of the light wave in the  $x$  axis. One important observation must be mentioned: The plane of the polarization is still maintained in the light output along the  $x$  axis in spite of the fact that the photon which travels through the resonance tube would be expected to experience many absorptions and re-emissions.

Finally, we will present some results on the light source when modulated with a square wave. Figures 10(a) and (b) show the light output obtained simultaneously on the  $x$  and  $y$  axes, respectively. The features of the two traces are quite different. We can find a kind of damping oscillatory overshoot in the light output on the  $x$  axis, while there is a typical delayed exponential response on the  $y$  axis.

### CONCLUSIONS

The transfer properties of resonance radiation measured in this experiment may furnish a new basis for test of existing theories. It is not evident at the moment whether these results are embraced by theory in its present form.

## Lifetimes of the $(5p^56s)^1P_1$ and $^3P_1$ States of Xenon\*†

D. KENT ANDERSON‡

*Department of Physics, University of Chicago, Chicago, Illinois*

(Received 3 August 1964)

The lifetimes of the  $(5p^56s)^3P_1$  and  $^1P_1$  states of Xe were measured by the zero-field level-crossing method (Hanle effect). The lifetimes are  $\tau(^3P_1) = 3.79 \pm 0.12 \times 10^{-9}$  sec and  $\tau(^1P_1) = 3.17 \pm 0.19 \times 10^{-9}$  sec. The corresponding oscillator strengths are  $^3f = 0.256 \pm 0.008$  and  $^1f = 0.238 \pm 0.015$ . The sum  $^1f + ^3f$  for the rare gases Ne to Xe is now known. The intermediate coupling coefficients derived from the lifetime ratio are in agreement with the theory of Wolfe, but not with that of Breit and Wills.

### INTRODUCTION

ATOMIC lifetimes are of general interest because of their intimate connection with the coupling of excited states to the radiation field. The lifetimes of the first few excited states are especially important in evaluating properties such as the polarizability, index of refraction, and van der Waals coefficient.<sup>1</sup> The latter is of particular interest in the case of the rare gases.<sup>2</sup>

\* This work was assisted by grants from the Sloan Foundation, National Science Foundation, and Advanced Research Projects Agency.

† Presented as a thesis to the Department of Physics, University of Chicago, in partial fulfillment of the requirements for the Ph.D. degree.

‡ Present address: Department of Physics, Montana State College, Bozeman, Montana.

<sup>1</sup> A. Dalgarno, *Rev. Mod. Phys.* **35**, 522 (1963).

<sup>2</sup> A. E. Kingston *Phys. Rev.* **135**, A1018 (1964).

The cross section for small-angle inelastic electron scattering from atoms and molecules also depends on the lifetimes through the corresponding oscillator strengths.<sup>3,4</sup>

In the solid state, the resonance lines of Xe are observed in absorption.<sup>5</sup> Similar structure is observed in the ultraviolet absorption spectrum of the alkali iodides,<sup>6</sup> where the iodide ion is isoelectronic to Xe.

The zero-field level crossing (Hanle effect) method has been used recently to measure the excited state

<sup>3</sup> E. N. Lassettre and E. A. Jones, *J. Chem. Phys.* **40**, 1222 (1964).

<sup>4</sup> J. Geiger, *Z. Physik* **177**, 138 (1963).

<sup>5</sup> G. Baldini, *Phys. Rev.* **128**, 1562 (1962).

<sup>6</sup> J. E. Eby, K. J. Teegarden, and D. B. Dutton, *Phys. Rev.* **116**, 1099 (1959).

lifetimes of several metallic elements.<sup>7-9</sup> Unfortunately, the resonance lines of the rare gases are in the vacuum ultraviolet region of the spectrum, where special optical techniques are required. However, the handicap of low intensity imposed by the unavailability of suitable lenses and filters can be overcome by using sensitive low-noise detection schemes.

### THEORY

Level crossings involving resonance fluorescence are observed experimentally by noting a change in the polarization or angular distribution of radiation from atoms excited by resonant absorption, as a function of an applied magnetic field. Zero-field crossings were first observed by Hanle<sup>10</sup> in experiments on the 2537-Å resonance line of Hg. The results of these experiments can be described by a classical theory of damped oscillating dipoles precessing with their Larmor frequency<sup>11,8</sup> or by a quantum-mechanical theory of interference effects in resonance fluorescence due to Breit.<sup>12</sup> This theory has been discussed by several authors<sup>13,14</sup> following the experimental observation of level crossing in He.<sup>15</sup> The Breit formula is presented in the Appendix, where the results for even isotopes are obtained.

For unpolarized resonance radiation and mutually perpendicular incoming beam, outgoing beam, and magnetic field, the resonance fluorescence intensity as a function of the magnetic field for a  $J=0 \leftrightarrow J=1$  transition is

$$I \propto \left[ \frac{1 + \frac{1}{2} \frac{(2\tau\omega)^2}{1 + (2\tau\omega)^2}}{1 + (2\tau\omega)^2} \right] \quad (1)$$

$$\omega = g\omega_L, \quad \omega_L = eH/2mc \text{ (Larmor frequency),}$$

where  $\tau$  and  $g$  are the lifetime and the  $g$  value of the excited state, respectively. If the  $g$  value is known, the lifetime is found from the value of  $H$  at half-maximum, where

$$\tau = (2\omega)^{-1} = mc/egH_{1/2}. \quad (2)$$

The  $g$  values for Xe are known from Zeeman effect measurements.<sup>16</sup> For the two  $J=1$  excited states of the  $5p^56s$  configuration, the  $g$  values are  $g(^3P_1) = 1.204(2)$  and  $g(^1P_1) = 1.321(10)$ , where the uncertainties are estimated from the spread in the measured Zeeman patterns.

<sup>7</sup> A. Landman and R. Novick, Phys. Rev. **134**, A56 (1964).

<sup>8</sup> A. Lurio, R. L. deZafra, and R. J. Goshen, Phys. Rev. **134**, A1198 (1964).

<sup>9</sup> A. Lurio and R. Novick, Phys. Rev. **134**, A608 (1964).

<sup>10</sup> W. Hanle, Z. Physik **30**, 93 (1924).

<sup>11</sup> A. C. G. Mitchell and M. W. Zemansky, *Resonance Radiation and Excited Atoms* (Cambridge University Press, New York, 1961).

<sup>12</sup> G. Breit, Rev. Mod. Phys. **5**, 91 (1933).

<sup>13</sup> P. A. Franken, Phys. Rev. **121**, 508 (1961).

<sup>14</sup> M. E. Rose and R. L. Carovillano, Phys. Rev. **122**, 1185 (1961).

<sup>15</sup> F. D. Colegrove, P. A. Franken, R. R. Lewis, and R. H. Sands, Phys. Rev. Letters **3**, 420 (1959).

<sup>16</sup> J. B. Green, E. H. Hurlburt, and D. W. Bowman, Phys. Rev. **59**, 72 (1941).

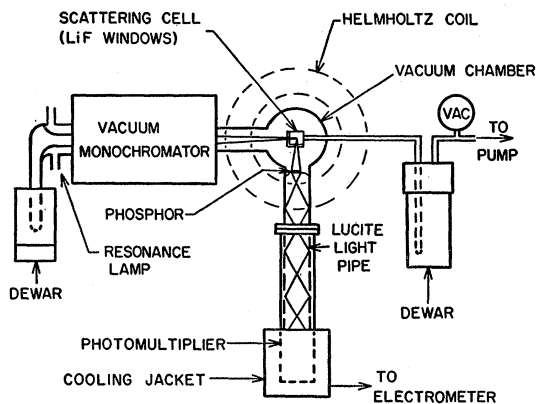


FIG. 1. Apparatus schematic.

### EXPERIMENTAL PROCEDURE

Light from a Xe resonance lamp was passed through a vacuum monochromator so that the resonance line illuminated the entrance window of a scattering cell mounted in a vacuum chamber (see Fig. 1). The fluorescence was viewed through the exit window at  $90^\circ$  to the collimated beam from the monochromator. A pair of Helmholtz coils provided a magnetic field perpendicular to the incoming and outgoing beams. The object was to measure the resonance fluorescence as a function of magnetic field for several different pressures in the scattering cell. The half-widths in gauss of the resulting Lorentzian line shapes were converted to apparent lifetimes and extrapolated to zero pressure.

### APPARATUS

The Xe resonance spectrum was obtained from an air-cooled microwave powered discharge lamp. It was equipped with a lithium fluoride window 1 mm thick and 20 mm in diameter, which was sealed to the lamp with a very thin layer of Apiezon W wax. A side arm of the lamp enabled the vapor pressure of the Xe to be controlled by cooling with liquid air. Typically, a lamp would be filled with Ne at a pressure of  $\sim 2$  Torr and  $\sim 1$  Torr of Xe, after purging the lamp with repeated Ne discharges. The lamp was sealed, and a barium getter flashed in the side arm. A mixture of liquid oxygen and liquid nitrogen in a Dewar flask was adjusted to give a Xe partial pressure in the range 0.002 to 0.01 Torr. At higher Xe pressures, the resonance lines became partially self-reversed as indicated by an increase in the total fluorescence without a corresponding increase in field-dependent signal.

The microwave power was provided by a Raytheon Microtherm magnetron oscillator operating at 2450 Mc/sec. The discharge was maintained in contact with the window so as to provide a thin emitting layer. This procedure was helpful in avoiding self reversal, but limited the useful operating life of the lamp to  $\sim 15$  h because of window contamination.

The resonance lines were selected by a Jarrel-Ash half-meter vacuum monochromator of the Seya-Namioka type. This largely eliminated background due to scattered visible light and allowed the beam entering the scattering cell to be well collimated. The slits on the monochromator were opened to several millimeters for maximum intensity, as the spectrum of the lamp consisted mainly of the Xe resonance lines from 1600 to about 1050 Å.<sup>17</sup>

The scattering cell was constructed of Pyrex with lithium fluoride windows 20 mm in diameter. A side arm of the cell was placed in a Dewar flask with a vacuum cap so that the vapor pressure of liquid nitrogen in the Dewar flask could be reduced by pumping. The pressure in the Dewar flask was measured with a mercury manometer and converted to temperature by consulting vapor pressure tables for the liquid and solid phases<sup>18,19</sup> of nitrogen. The corresponding vapor pressure of Xe was computed from data given by Dushman.<sup>20</sup>

The detector consisted of a light pipe and an E.M.I. 9514B photomultiplier tube. A thin layer of sodium salicylate was deposited on the end of a polished Lucite rod.<sup>21</sup> The tip was shaped so that all light entering the rod from the phosphor would be totally reflected to the face of the photomultiplier. The light pipe was needed to remove the photomultiplier from the magnetic field. The detector assembly was mounted in a vacuum-tight brass housing to facilitate cooling the photomultiplier with dry ice. This chamber was separated from the monochromator by an O-ring seal and filled with dry air. Cooling the detector in this manner reduced the dark current by more than two orders of magnitude, so that it was a fraction of the signal. The photomultiplier current was measured by an electrometer.

The current through the Helmholtz coil was determined by measuring the voltage across a 1-Ω precision resistor with a Fluke 825A differential voltmeter. The coil was calibrated by comparing it to a low-field proton resonance probe by means of a differential gaussmeter.

TABLE I. Operating conditions at 1470 Å with natural isotopic abundance.

Photomultiplier gain	10 <sup>6</sup>
Dark current	10 <sup>-10</sup> A
Xe pressure in cell	4×10 <sup>-6</sup> Torr
Instrumental scattering	4×10 <sup>-9</sup> A
Fluorescence at zero field	2×10 <sup>-9</sup> A
Field-dependent signal	4×10 <sup>-10</sup> A
Signal/noise	10

<sup>17</sup> Fluorescence at 1250 and 1192 Å ( $5p^6 \rightarrow 5p^55d$ ) was also observed.

<sup>18</sup> W. H. Keesom and A. Bijl, *Physica* 4, 305 (1937).

<sup>19</sup> G. T. Armstrong, *J. Res. Natl. Bur. Std. (U. S.)* 53, 263 (1954).

<sup>20</sup> S. Dushman, *Scientific Foundations of Vacuum Technique* (John Wiley & Sons, Inc., New York, 1962), 2nd ed., p. 728.

<sup>21</sup> I am indebted to P. M. McPherson for suggesting the use of sodium salicylate in conjunction with a light pipe.

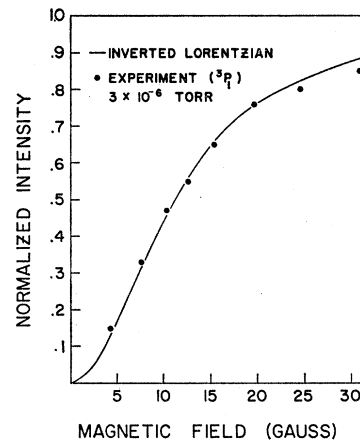


FIG. 2. Line shape for 1470-Å fluorescence from even isotopes.

The calibration constant was  $1.67 \pm 0.01$  G/mA, and the magnetic field variation over the cell volume was  $\pm 0.5\%$ . The earth's magnetic field contributed 0.4 G perpendicular to the axis of the coil.

## RESULTS

Preliminary experiments were performed using Xe of natural isotopic abundance to determine the best operating conditions. The cell was evacuated to measure instrumental scattering. A typical set of operating conditions is given in Table I. For the final experiments a mixture of enriched isotopes<sup>22</sup> containing 99.4% even isotopes was used in the lamp as well as in the cell. This was necessary to avoid hyperfine structure complications, and the use of even isotopes raised the signal-to-noise ratio by a factor of 3. Isotopic abundances are presented in Table II.

The half-width was determined by fitting a Lorentzian curve to the normalized intensity. One such line shape for even isotopes is shown in Fig. 2. The line shape is in good agreement with theory up to twice the half-width. The deviation in the wings of the line may be due to scanning the shoulder of the Doppler broadened line from the lamp, causing a decrease in scattered intensity. The possible asymmetry in the signal due to deviations from a  $\pi/2$  scattering angle was estimated to be 1% or less by reversing the magnetic field. The use of a collimated beam from a monochromator rather than the usual case of highly convergent beams from large aperture lenses made the optical geometry more certain.

TABLE II. Isotopic composition.

Isotope of Xe	129	131	132	134	136
% Abundance (natural)	26.24	21.24	26.93	10.52	8.93
% Abundance (enriched)	...	0.60	2.00	14.43	82.96
Nuclear spin	$\frac{1}{2}$	$\frac{3}{2}$	0	0	0

<sup>22</sup> The isotopes were obtained from Monsanto Research Corporation, Mound Laboratory, Miamisburg, Ohio.

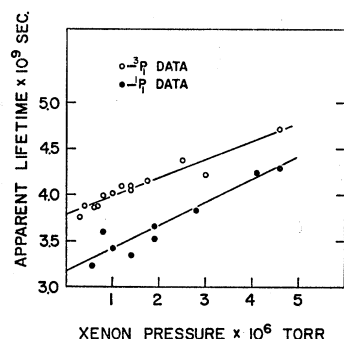


FIG. 3. Extrapolation of apparent lifetimes to zero pressure.

The half-widths were measured at various pressures and extrapolated to zero pressure as shown in Fig. 3, where the half-widths are given in terms of apparent lifetimes. The signal at 1296 Å ( $^1P_1$  line) was less intense than the signal at 1470 Å ( $^3P_1$  line) due to the smaller output of the lamp and reduced grating efficiency of the monochromator. The extrapolated values of  $H_{1/2}$  were

$$H_{1/2}(^3P_1) = 12.46 \pm 0.37 \text{ G},$$

$$H_{1/2}(^1P_1) = 13.58 \pm 0.81 \text{ G}.$$

The lifetimes calculated from Eq. (2) are

$$\tau(^3P_1) = 3.79 \pm 0.12 \times 10^{-9} \text{ sec},$$

$$\tau(^1P_1) = 3.17 \pm 0.19 \times 10^{-9} \text{ sec}.$$

The uncertainties quoted are three times the rms deviation as determined by a least-squares fit. They include the uncertainties due to field measurement, asymmetry effects, and  $g$  values. A similar extrapolation of preliminary data for Xe of natural isotopic abundance gave  $H_{1/2}(^3P_1) = 20 \pm 2 \text{ G}$ .

## DISCUSSION

### A. Preliminary Experiments

From Table I, the experiment on Xe of natural isotopic abundance gives a ratio of field-dependent signal to total fluorescence at zero field equal to 0.20. The theory for the even isotopes predicts a ratio of 0.50, but the corresponding ratio for the odd isotopes is smaller. For  $\text{Xe}^{129}$  with  $I = \frac{1}{2}$ , the theoretical expression given by Lurio and Novick<sup>9</sup> gives 0.14 and the ratio for  $\text{Xe}^{131}$  with  $I = \frac{3}{2}$  should be even smaller, due to the smaller proportion of levels available for interference. The ratio of field-dependent signal to total fluorescence at zero field was 0.25 at cell pressures less than  $10^{-6}$  Torr, which agrees with the ratio calculated from the natural isotopic abundances, if it is assumed that the contribution from  $\text{Xe}^{131}$  was negligible.

Another effect of the odd isotopes is the distortion of the line shape due to the many hyperfine  $g_F$  values. In an earlier report<sup>23</sup> on the measurement of the Hanle

<sup>23</sup> D. Anderson and W. Lichten, *Bull. Am. Phys. Soc.* **9**, 65 (1964).

effect of the 1470-Å line, the large uncertainty in the resulting lifetime was due to the uncertainty of the odd isotope effects. Since  $H_{1/2}$  has been measured for the even isotopes the ratio of the two fields can be used to define an "average"  $g_F$ ,  $\langle g_F \rangle_{\text{av}} = 0.63 \pm 0.07 g_J$ , for the natural mixture of isotopes. This "average" value is not a true average for two reasons. The line shape is not strictly Lorentzian, and not all the hyperfine levels contribute to the field-dependent signal.

### B. Oscillator Strengths

The oscillator strength  $f$  is related to the lifetime by<sup>8,11</sup>

$$f\tau = \frac{mc}{8\pi^2 e^2} \frac{g_2}{g_1} \lambda^2 = 1.499 \frac{g_2}{g_1} \lambda^2, \quad (3)$$

where  $g_1 = 1$  and  $g_2 = 3$  are the statistical weights of the ground state and the excited state, respectively. ( $\tau$  is in seconds if  $\lambda$  is in centimeters.) The resulting oscillator strengths are

$$^3f = 0.256 \pm 0.008, \quad ^1f = 0.238 \pm 0.015.$$

The sum of the oscillator strengths for the resonance lines of the rare gases show a remarkably regular increase from Ne to Xe. This is illustrated in Fig. 4. Gold and Knox have calculated the  $f$  values for  $^{24}\text{Ne}$  and  $\text{Ar}$ .<sup>25</sup> The experimental values for Ne, Ar, and Kr reported by Geiger<sup>4</sup> are derived from small-angle, inelastic electron scattering cross sections. The triplet oscillator strength of Xe is in agreement with the value  $^3f = 0.263$  given by Geiger in his thesis.<sup>26</sup>

The ratio of triplet and singlet oscillator strengths can be calculated from expressions given by Knox<sup>25</sup> and compared to the experimental ratio. The theory gives  $^3f/^1f = 1.10$  which agrees with the experimental ratio  $^3f/^1f = 1.08 \pm 0.07$ .

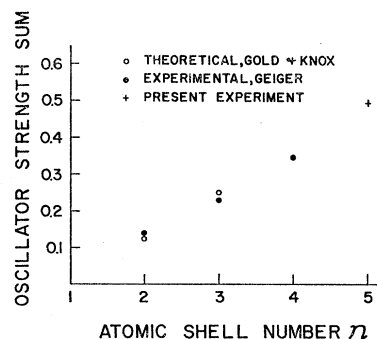


FIG. 4. Oscillator strength sum for the resonance lines of the rare gases Ne-Xe. References:  $\circ$ —A. Gold and R. Knox, *Phys. Rev.* **113**, 834 (1959); R. Knox, *Phys. Rev.* **110**, 375 (1958);  $\bullet$ —J. Geiger, *Z. Physik* **177**, 138 (1963).

<sup>24</sup> A. Gold and R. Knox, *Phys. Rev.* **113**, 834 (1959).

<sup>25</sup> R. Knox, *Phys. Rev.* **110**, 375 (1958).

<sup>26</sup> J. Geiger, thesis, Technical University of Berlin, 1962 (unpublished).

TABLE III. Intermediate coupling coefficients.

	$\alpha$	$\beta$	$C_1$	$C_2$
Lifetime ratio	0.671	0.742	0.993	0.119
Wolfe	0.664	0.748	0.994	0.111
$g(^3P_1)$	0.639	0.770	0.997	0.077
$g(^1P_1)$	0.598	0.801	0.999	0.026

### C. Intermediate Coupling

The ratio of the lifetimes may be used to determine the intermediate coupling coefficients,  $\alpha$ ,  $\beta$ ,  $C_1$ ,  $C_2$ , defined by

$$\psi(^3P_1) = C_1 \left(\frac{3}{2}, \frac{1}{2}\right)_1 + C_2 \left(\frac{1}{2}, \frac{1}{2}\right)_1 = \alpha \psi(^3P_1^0) + \beta \psi(^1P_1^0), \quad (4)$$

where  $\left(\frac{3}{2}, \frac{1}{2}\right)_1$  and  $\left(\frac{1}{2}, \frac{1}{2}\right)_1$  are pure  $(j j)$  coupled states.  $\psi(^3P_1^0)$  and  $\psi(^1P_1^0)$  are pure Russel-Saunders states. The lifetime ratio gives<sup>27</sup>

$$\frac{\beta^2}{\alpha^2} = \frac{\tau(^1P_1)\lambda^3(^3P_1)}{\tau(^3P_1)\lambda^3(^1P_1)}, \quad \alpha^2 + \beta^2 = 1, \quad (5)$$

where  $\lambda$  is the wavelength of the appropriate resonance line.

There are various methods for estimating the coupling coefficients from atomic properties other than the lifetimes. Breit and Wills<sup>28</sup> give them in terms of the  $g$  values.

$$\begin{aligned} \beta^2 &= 2[g(^1P_1) - 1], \\ \alpha^2 &= 2[g(^3P_1) - 1]. \end{aligned} \quad (6)$$

The theory of multiplet splitting due to Wolfe<sup>29</sup> gives

$$\beta^2 = \frac{2[E(^3P_1) - E(^3P_0)] - [E(^3P_2) - E(^3P_1)]}{3[E(^3P_1) - E(^1P_1)]}, \quad (7)$$

where  $E(^3P_J)$  is the spectroscopic term value (see Fig. 5). The resulting values of the coupling coefficients are presented in Table III.

The coefficients derived from the  $g$  values are in disagreement with the others, as well as with each other. However, it is to be noted that the  $g$ -sum rule is

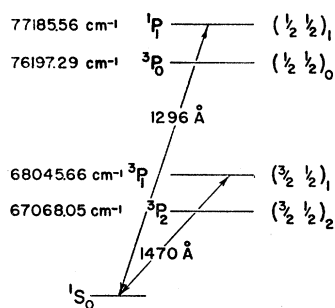


FIG. 5. Energy levels of the  $5p^6 6s$  configuration in Xe.

<sup>27</sup> A. Lurio, M. Mandel, and R. Novick, Phys. Rev. 126, 1758 (1962).

<sup>28</sup> G. Breit and L. A. Wills, Phys. Rev. 44, 470 (1933).

<sup>29</sup> H. C. Wolfe, Phys. Rev. 41, 443 (1932).

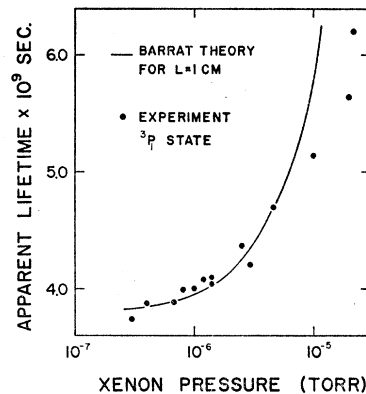


FIG. 6. Apparent lifetime versus cell pressure.

not obeyed for this configuration in Xe,<sup>16</sup> so the method is probably not reliable in this case. The theory of Wolfe has three parameters to be fixed by the term values and agrees with the coefficients derived from the lifetimes.

### D. Coherence Narrowing

The previously mentioned theories<sup>12,13</sup> assume that the resonance photon is scattered from the atom directly to the detector. If the atom density in the scattering cell is high enough, there will be a finite chance of scattering more than once. The effect of multiple diffusion of resonance photons has been investigated theoretically by Barrat<sup>30</sup> with the result that the true radiative lifetime  $\tau$  is related to the observed lifetime or "coherence time"  $T$  by

$$T/\tau = (1 - \alpha x)^{-1}, \quad (8)$$

where  $x$  is the probability that a photon emitted by an atom in the cell will be absorbed once more before it escapes. The expression for  $x$  can be written

$$x = 1 - \exp(-\sigma n L), \quad (9)$$

where  $n$  = atom density,  $L$  = typical cell dimension, and  $\sigma$  is a cross section given by

$$\sigma = (\pi/2) r_0 \lambda f c / \bar{v}. \quad (10)$$

In Eq. (10),  $\lambda$  is the wavelength,  $f$  is the oscillator strength,  $r_0$  is the classical electron radius, and  $\bar{v}$  is the average thermal velocity. The parameter  $\alpha$  is a fraction less than one that depends on the particular isotope. This theory agrees moderately well with the data, but begins to deviate at higher pressures. The data for even isotopes at 1470 Å are compared to the theory for  $L = 1$  cm in Fig. 6.

### ACKNOWLEDGMENTS

I wish to thank Professor W. L. Lichten for suggesting this problem, and for his advice and encouragement. I am indebted to R. T. Robiscoe for valuable discussions,

<sup>30</sup> J. P. Barrat, J. Phys. Radium 20, 541, 633, 657 (1959).

and to J. F. Bolton and M. Machalek for laboratory assistance. Finally, I wish to thank the staff of Ryerson Physical Laboratory, and Professor R. S. Mulliken and M. L. Ginter for the use of the spectroscopic facilities of the Laboratory for Molecular Structure and Spectra.

### APPENDIX

The Breit formula<sup>12</sup> gives the rate at which photons of polarization  $\mathbf{f}$  are absorbed and photons of polarization  $\mathbf{g}$  are re-emitted in resonance fluorescence. The rate is

$$R(\mathbf{f} \mathbf{g}) = C \sum_{\mu\mu', mm'} \frac{f_{\mu m} f_{\mu' m'} g_{\mu' m'} g_{\mu m}}{1 - i\tau\omega(\mu, \mu')}, \quad (1B)$$

where  $m, m'$  are ground-state levels and  $\mu, \mu'$  are excited-state levels indicated by their magnetic quantum numbers. The matrix elements

$$f_{\mu m} = (\mu | \mathbf{f} \cdot \mathbf{r} | m), \quad g_{\mu m} = (\mu | \mathbf{g} \cdot \mathbf{r} | m)$$

are the dipole matrix elements involved in the transitions. The mean lifetime of the excited state is  $\tau$ ,  $\omega(\mu, \mu') = (E_\mu - E_{\mu'})/\hbar$ , and  $C$  is a factor proportional to the intensity, geometrical factors, etc.

The simplest application of this formula is resonance scattering from a  $J=0$  ground state to a  $J=1$  excited state, as in the case of the rare-gas isotopes of zero nuclear spin. For the nondegenerate ground state  $^1S_0$ ,  $m = m' = 0$ .

$$R = \sum_{\mu\mu'} \frac{f_{\mu 0} f_{0\mu'} g_{\mu' 0} g_{0\mu}}{1 - i\tau\omega(\mu, \mu')}, \quad (2B)$$

where  $\omega(\mu, \mu') = (\mu - \mu') g_J (eH/2mc) = \Delta\mu\omega$ ,  $C=1$ . The values  $\mu, \mu'$  range over  $-1, 0, +1$ , so there are nine terms in the sum.

The nine terms are

$$\begin{aligned} R = & f_{10} f_{01} g_{10} g_{01} + \frac{f_{10} f_{00} g_{00} g_{01}}{1 - i\omega\tau} + \frac{f_{10} f_{0-1} g_{-10} g_{01}}{1 - i2\omega\tau} \\ & + \frac{f_{00} f_{01} g_{10} g_{00}}{1 + i\omega\tau} + f_{00} f_{00} g_{00} g_{00} + \frac{f_{00} f_{0-1} g_{-10} g_{00}}{1 - i\omega\tau} \\ & + \frac{f_{-10} f_{01} g_{10} g_{0-1}}{1 + i2\omega\tau} + \frac{f_{-10} f_{00} g_{00} g_{0-1}}{1 + i\omega\tau} + f_{-10} f_{0-1} g_{-10} g_{0-1}. \end{aligned} \quad (3B)$$

The polarization vectors for the case of incoming

radiation along the  $y$  axis and outgoing radiation along the  $x$  axis are

$$\mathbf{f} = \mathbf{i} \cos\vartheta_1 + \mathbf{k} \sin\vartheta_1, \quad \mathbf{g} = \mathbf{j} \cos\vartheta_2 + \mathbf{k} \sin\vartheta_2.$$

The matrix elements for  $f_{\mu m}$  are

$$\begin{aligned} f_{0-1} &= \mathbf{f} \cdot (1/\sqrt{2})(\mathbf{i} - \mathbf{j}), \\ f_{01} &= -\mathbf{f} \cdot (1/\sqrt{2})(\mathbf{i} + \mathbf{j}), \\ f_{00} &= f_{11} = f_{-1-1} = \mathbf{f} \cdot \mathbf{k}, \end{aligned} \quad (4B)$$

and similarly for  $g_{\mu m}$ . Explicitly, the sum is

$$\begin{aligned} R &= \sum_{i=1}^9 R_i. \\ R_1 &= f_{10} f_{01} g_{10} g_{01} = (1/4) \cos^2\vartheta_1 \cos^2\vartheta_2 = R_9, \\ R_2 &= \frac{f_{10} f_{00} g_{00} g_{01}}{1 - i\omega\tau} = (i/2) \frac{\cos\vartheta_1 \sin\vartheta_1 \cos\vartheta_2 \sin\vartheta_2}{1 - i\omega\tau} \\ &= R_6 = R_4^* = R_8^*, \\ R_3 &= \frac{f_{10} f_{0-1} g_{-10} g_{01}}{1 - i2\omega\tau} = -(1/4) \frac{\cos^2\vartheta_1 \cos^2\vartheta_2}{1 - i2\omega\tau} = R_7^*, \\ R_5 &= f_{00} f_{00} g_{00} g_{00} = \sin^2\vartheta_1 \sin^2\vartheta_2. \end{aligned} \quad (5B)$$

The average over polarization gives

$$\langle \cos^2\vartheta_i \rangle_{av} = \langle \sin^2\vartheta_i \rangle_{av} = \frac{1}{2}, \quad \langle \cos\vartheta_i \sin\vartheta_i \rangle_{av} = 0.$$

Thus,

$$\bar{R} = \left(\frac{1}{4}\right) \left[ 1 + \frac{1}{2} \frac{(2\omega\tau)^2}{1 + (2\omega\tau)^2} \right]. \quad (6B)$$

The field-dependent signal comes from  $R_3$  and  $R_7$ . For example,

$$R_3 = \frac{(f_{10} g_{01})(f_{0-1} g_{-10})}{1 - i2\omega\tau}. \quad (7B)$$

The numerator can be interpreted as the product of amplitudes for an  $m=0 \rightarrow \mu=\pm 1$  absorption followed by a re-emission. Consequently, this term represents the interference between the  $\mu=\pm 1$  upper states.

Pictorially, the  $\mu=\pm 1 \rightarrow m=0$  transitions give photons circularly polarized in opposite directions, and their interference gives linearly polarized light. This interference is rendered ineffective by the magnetic field because the linear vibration then has a rapidly precessing axis.